

DEVELOPMENT OF SOFC TECHNOLOGY AT TAIWAN INSTITUTE OF NUCLEAR ENERGY RESEARCH

Ruey-Yi Lee, Yung-Neng Cheng, Tai-Nan Lin, Chang-Sing Hwang, Ning-Yih Hsu, Wen-Tang Hong and Chien-Kuo Liu

Institute of Nuclear Energy Research, Taoyuan, Taiwan, R.O.C.

ABSTRACT

Taiwan Institute of Nuclear Energy Research (INER) has committed to developing the SOFC technology since 2003. Since then, substantial progresses have been made on cell, sealant, stack, reforming catalyst, balance of plant (BOP) components as well as system integration. To date, fabrication processes for both planar anode-supported-cell (ASC) by conventional methods and metal-supported-cell (MSC) by atmospheric plasma spraying have been well established. Numerous stack tests were carried out with consistent and repeatable results. Several thousand hours performance tests were executed to evaluate the reliability and durability of system components. Recently, a compact INER-III SOFC power system has been demonstrated with an electric efficiency higher than 40%.

INTRODUCTION

The merits of Solid Oxide Fuel Cell (SOFC) include high efficiency, module design, insignificant NO_x, SO_x and particulate emissions, reduced CO₂ emissions, fuel flexibility as well as vibration-free operation. Nowadays, the SOFC is considered as an environmentally friendly energy-converting device and an essential bridge from the fossil fuel to the next generation power systems. For the past decade, the INER has imposed critical mass and substantial efforts to develop the core technology of the SOFC technology from powder to power. Elaborative efforts have been made in parallel to the membrane electrode assembly (MEA), stack and power system developments.¹⁻⁶ Firmed facilities for hardware and software are sequentially set up to move forward the SOFC technology development. A series of MEA and short stack tests have been conducted to evaluate the cell/stack performance for further improvement and to find out the key operational parameters. In 2007, the first home-made MEA with a maximum power density higher than 500 mW/cm² was fabricated. At the end of 2007, the first 1kW stack with InDec cells inside was assembled and tested with success. In November of 2008, through a close international collaboration between INER and HTceramix SA, over 1000-hour performance test of the HTc's long stack in the INER's test facility was carried out with an electric output over 1 kW. A prototype of INER's first 1-kW SOFC power system with natural gas as fuel was illustrated thermally self-sustaining at the last week of 2011. The system was then transferred to the China Steel Cooperation (CSC) for further in-situ testing. A durability test over 15,000 hours for INER's ASC cell under a constant current density of 400 mA/cm² with a degradation rate of about 1%/khr was fulfilled in 2012. A technology transfer on the fabrication processes of the SOFC MEA was signed to a local fine ceramic company in January of 2014. Through the system integration of hot components of the balance of plant, the second generation of INER-II with a system volume reduction of 55% compared to the first prototype was demonstrated and transferred to the China Petroleum Cooperation in 2013. A further system volume reduction of 20% for a compact INER-III power system with satisfactory electric efficiency was achieved in 2015. In this paper, developments of MEA (ASC and MSC), high temperature seals, stack and system at INER are updated.

MEA DEVELOPMENT

For the INER ceramic anode supported cells (ASCs), efforts have been devoted in the total solution of preparing the commercial-available cell products in the past decade. For the starting materials, the patented glycine nitrate combustion (GNC) reactor can be used for preparation of novel electrode/electrolyte in kg-scale.⁷ Selected materials for anode, electrolyte, and cathode are (NiO-YSZ ($Y_{0.08}Zr_{0.92}O_{2-\delta}$) (8 mol% yttria-stabilized-zirconia)), (NiO-SDC ($Sm_xCe_{1-x}O_{2-\delta}$)), (NiO-LSGM ($La_{1-x}Sr_xGa_{1-y}Mg_yO_{3-\delta}$)), CMF ($Ce_xMn_yFe_{1-x-y}O_2$); YSZ, SDC, LSGM, BYCZ ($BaY_xCe_yZr_{1-x-y}O_{3-\delta}$), NBT ($Na_{0.5}Bi_{0.49}Ti_{0.98}Mg_{0.02}O_3$); LSM ($La_{1-x}Sr_xMnO_{3-\delta}$), LSCF ($La_{1-x}Sr_xCo_yFe_{1-y}O_{3-\delta}$), LSC ($La_{1-x}Sr_xCo_yO_{3-\delta}$), BSCF ($Ba_{1-x}Sr_xCo_yFe_{1-y}O_{3-\delta}$), SSC ($Sm_xSr_{1-x}CoO_{3-\delta}$), and SBSC ($SmBa_xSr_{1-x}Co_2O_{5+\delta}$), respectively.⁵⁻¹¹ Of which, the subscript delta (δ) refers to the amount of oxygen deficiency extent in the specific ideal stoichiometric crystallinity, typically ranging from 0 to 0.1. For the ceramic support, anode and electrolyte tapes are fabricated via tape casting processes and laminated to form ceramic substrates (product dimension: $10 \times 10 \text{ cm}^2$, thickness: $100 \sim 550 \text{ }\mu\text{m}$). Thin film processing methods are utilized to fabricate individual layers in the SOFC MEA. Figure 1 illustrates the cell fabrication processing flow chart developed at INER. As for the 1st-gen INER-SOFC-MEA with traditional materials (NiO-YSZ|YSZ|YSZ-LSM|LSM), the performance has been proven to have long-term durability with about 1 %/khr degradation rate after 15000 hours operation at $800 \text{ }^\circ\text{C}$ as shown in Figure 2. The history of power, current, voltage, and temperature versus time is illustrated in the figure, and same Y-axis digital values (from 0 to 1000, in the unit of mW/cm^2 ; mA/cm^2 ; mV/cm^2 ; and $^\circ\text{C}$, respectively) were employed for each plot with different color and symbol. Further investigation on the structure stability of the cell after long term operation can be executed by STEM with phase identification.¹¹ Figures 3 and 4 indicated the cell's STEM images after 15,000-hour operation. Analyses of diffraction patterns were carried out to check the individual crystallinity of electrodes and electrolyte. The results indicated that no other crystalline phases existed after such a long-term cell operation. Additionally, the EDS results in Figures 3 and 4 indicated only slight diffusion for the electrode elements could be observed in the very shallow surfaces of the electrode/electrolyte interfaces, suggesting that the cell remain compositional stable. Structure modification in the anode with reduced thickness was carried out to enhance the cell performance to a higher power density. Furthermore, by introducing high catalytic cathode materials in the YSZ-based ASCs, like SSC or SBSC with perovskite structures, the P_{max} was increased to over $650 \text{ mW}/\text{cm}^2$ with slight degradation for 1000 hours operation as shown in Figure 5. Process optimizations in all areas are evaluated for improving the cell quality in fabricating the anode supported solid oxide fuel cell.

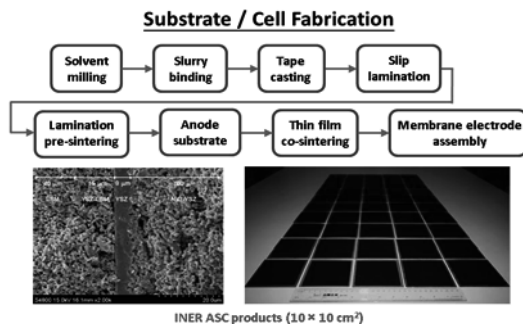


Figure 1. The INER-SOFC-MEA fabrication flow chart.

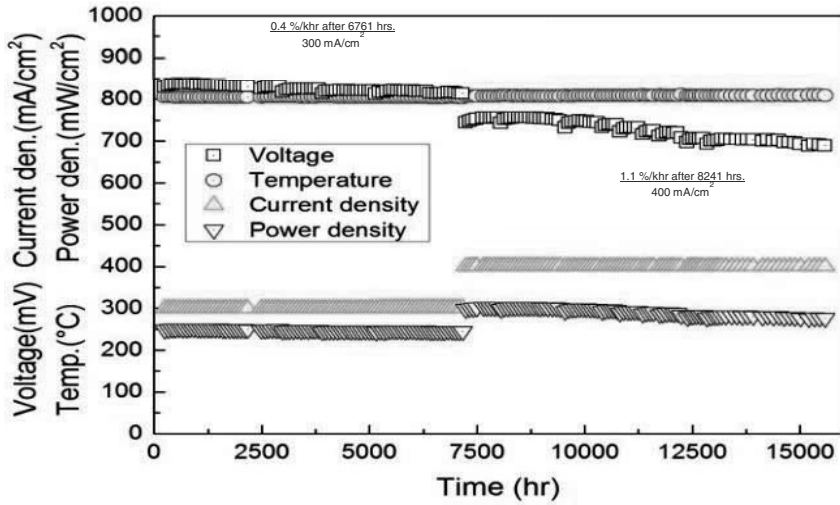


Figure 2. Long-term durability test result for 1st-gen INER-SOFC-MEA with cell structure of NiO-YSZ|YSZ|YSZ-LSM|LSM.

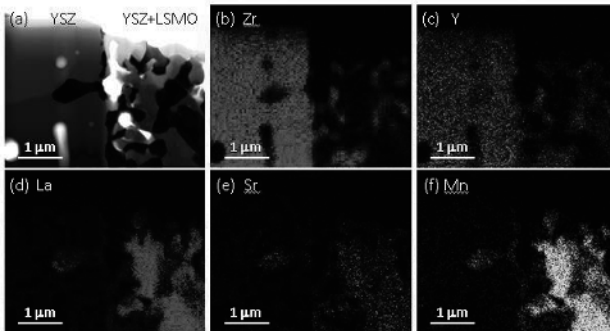


Figure 3. Composition analyses between electrolyte/cathode interfaces after 15000 hours operation.

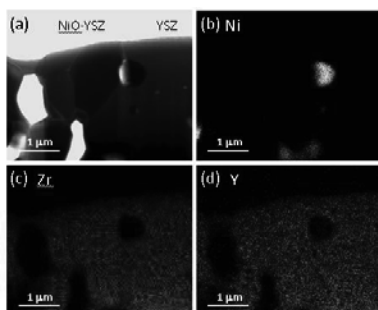


Figure 4. Composition analyses between anode/electrolyte interfaces after 15000 hours operation.

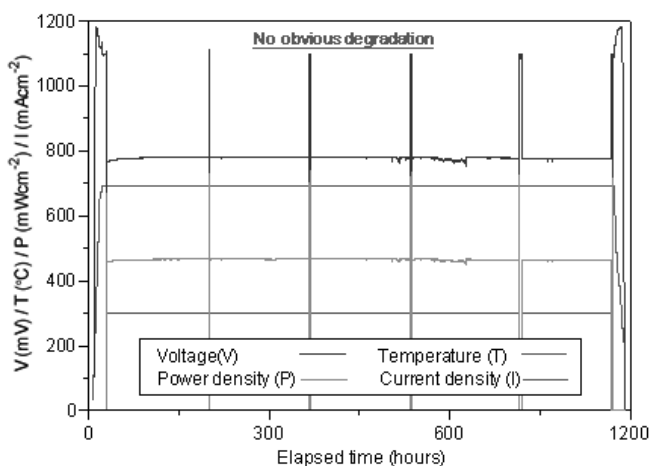


Figure 5. Durability result for ASC with perovskite series cathode material SBSC.

A planar Metal-Supported Solid Oxide Fuel Cell (MS-SOFC) composed of a novel Ni-based substrate, NiO-YSZ and NiO-LDC($\text{Ce}_{0.55}\text{La}_{0.45}\text{O}_{2.6}$) layers as double anode, a SDC($\text{Sm}_{0.15}\text{Ce}_{0.85}\text{O}_{3.6}$) layer as a diffusion barrier, a LSGM($\text{La}_{0.8}\text{Sr}_{0.2}\text{Ga}_{0.8}\text{Mg}_{0.2}\text{O}_{3.6}$) layer as an electrolyte and double layers with 50:50 wt% and 25:75 wt% of SDC and SSC($\text{Sm}_{0.5}\text{Sr}_{0.5}\text{CoO}_{3.6}$) to form composite coatings as a cathode with high power output, stability and thermal-shock abilities was successfully produced by the atmospheric plasma spraying (APS) process. A novel metal substrate with uniformly distributed straight gas flow channels of 0.8 mm in diameter and 0.5 mm in depth were fabricated in the bottom side of substrate. This kind of substrate facilitates gas inter-diffusion between hydrogen and water in the anode side of MS-SOFC cell so that hydrogen oxidation reactions can be effectively improved. Moreover, due to the fast sintering feature of APS technique, morphologies of anode and cathode layers remain their nano-structures and thus it provides large amount of triple phase boundaries, as shown in Figure 6(a), for anodic

and cathodic reactions to increase electricity output performance. The current-voltage-power (I-V-P) curves of a single INER-MS-SOFC unit cell at 750 and 700°C are shown in Figure 6(b). The open-circuit voltages higher than 1.0 V indicated that the LSGM electrolyte is dense enough. The maximum power densities were 593 and 510 mW/cm² at 750 and 700°C, respectively. The innovative type of MS-SOFC cell was then assembled to a single-cell stack for performance testing. Under the test conditions of 700°C and constant current density of 400 mA/cm², the degradation rate was about 0.77 %/khr, as shown in Figure 7.

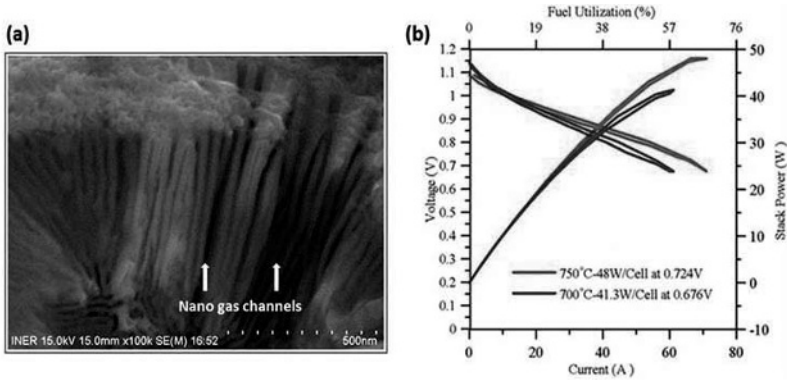


Figure 6. (a) Nano-channels in plasma sprayed Ni-YSZ anode. (b) I-V-P plots of INER-MS-SOFC single stack.

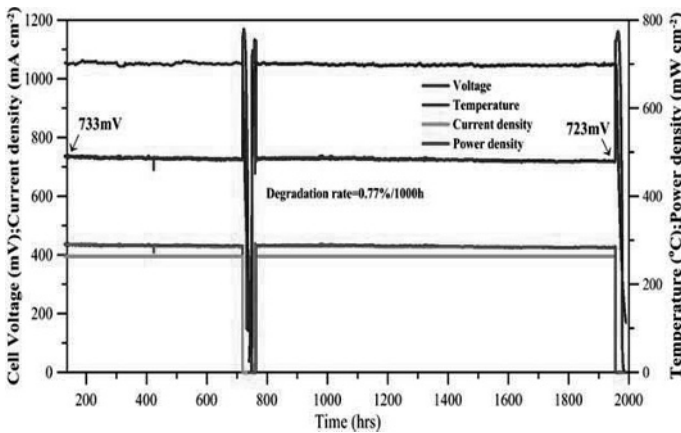


Figure 7. Long-term durability test results of an MS-SOFC single stack.

HIGH-TEMPERATURE SEALS DEVELOPMENT

Glass and glass-ceramic based materials are widely used as high-temperature seals due to its exceptional properties for SOFC stack.¹³⁻¹⁵ Several requirements have to be satisfied while a glass-ceramic sealant is employed in a SOFC stack, including coefficient of thermal expansion (CTE) compatible and chemical stable with other adjacent components and long-term thermal stability and durability at elevated temperatures (e.g. 650~900°C). A proprietary barium-aluminum-borosilicate glass, designated as GC9, as well as its paste formulation were developed by the Institute of Nuclear Energy Research (INER) for use as a high-temperature seals in SOFC applications.¹⁶⁻²¹ The glass transition (T_g), softening (T_s), and crystallization temperatures of GC9 glass are 652°C, 745°C, and 820°C, respectively. The CTE for the bulk and crystallized GC9 glass are 12.5 ppm/°C and 13.1 ppm/°C, respectively. Under an external loading of 0.08 MPa, the minimum viscosity, viscosity reflection point, and shrinkage percentage are 10^8 Pa·s, 806°C, and 64%, respectively. Figure 8(a) shows that the main crystalline phase of non-isothermally crystallized GC9 glass is $Ba_3La_6(SiO_4)_6$. However, as shown in Figure 8(b), it appears needle-like crystalline phase of $Ba(Al_2Si_2O_8)$ in the sintered form of GC9 powders. It is noted that an adequate glass/ceramic phase ratio (e.g. 0.50) can be obtained for the GC9 glass via non-isothermal crystallization, which is one of the key properties for keeping good wetting and gas tightness during sealing and operating processes for a SOFC stack. Additionally, the mechanical properties of GC9 glass sealant for use in SOFC applications have been systematically investigated and can be referred from elsewhere.²²⁻²⁸ We also introduced the phlogopite mica blending into GC9 glass powders and verified the improvement of the ductility of the sintered phlogopite mica/GC9 glass hybrid sealants. Furthermore, Figure 9 shows that the average leakage rates are 5.58×10^{-5} and 2.10×10^{-4} mbar·l/s/cm corresponding to the sealant of GC9 glass and GC9 glass/mica mixture, respectively.

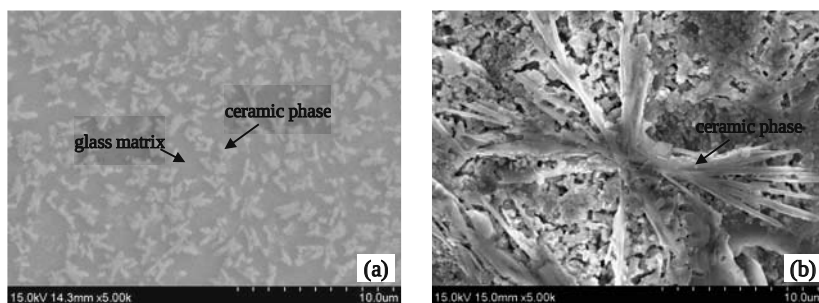


Figure 8. SEM Micrographs of (a) non-isothermally crystallized GC9 glass (bulk), and (b) sintered GC9 glass powders.

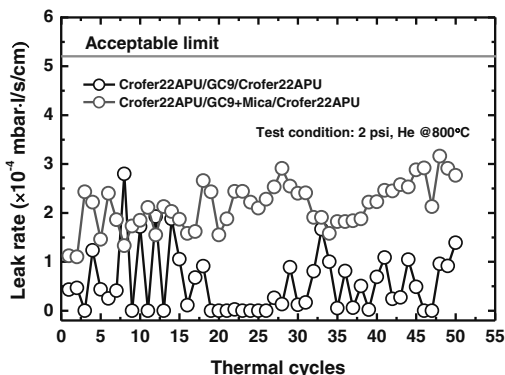


Figure 9. Leak rate of sealed Crofer22 APU/GC9 glass/Crofer22 APU and Crofer22 APU/GC9 glass + mica mixture/Crofer22 APU coupons during 50-thermal cycling test at 800°C in air.

STACK DEVELOPMENT

Standard operation procedures are well established and revised on a regular basis to obtain consistent test results and make further improvements. A series of cell/stack tests have been conducted to evaluate the cell/stack performance and effects of reduction processes as well as to find out the optimized operating conditions.²⁹⁻³¹ Electrochemical impedance spectroscopy was employed to characterize the electrical performance, lateral impedance as well as overall impedance spectrum of a cell or stack. The Taguchi method was applied to optimize the operating parameters for a cell/stack.³²⁻³³ Under the operating conditions of temperature 700 °C, the flow rate of cathode air at 2 liters per minutes (LPM), and the flow rate of hydrogen fuel in the anode varied from 0.2 to 1.4 LPM, a performance map, shown as Figure 10, for a single-cell stack was established. The operating parameters (fuel flow rate, voltage, current, power, fuel utilization and electric efficiency) and ranges for a single-cell stack are illustrated in Table 1. The performance map provides as a guideline for long-stack and system operations. For instance, if a stack is operated at the point A in the Figure 10, where the flow rate and current are at 605 sccm (standard cubic centimeter per minute) and 49 amperes, then its stack voltage, stack power, fuel utilization and power efficiency are correspondingly to 0.815 V, 40 W, 62% and 40%, respectively.

The essential features of current INER's SOFC stack are planar design, counter flow, internal manifold, metallic interconnect, and two-in-one-out layout in the anode and cathode compartments. The glass-ceramic sealants are used as high-temperature seals. Performance tests of 1-cell, 3-cell, and 5-cell stacks are sequentially carried out to validate the consistence and repeatability. A planar 36-cell stack composed of two end plates, 36 window frames, Crofer22 interconnects, and commercial cells was assembled and tested. The glass-ceramic GC9, validated its suitability by a long-term, single-cell stack functional test for over 6000 hours, was used as sealants. The test conditions for the stack were operating temperature 700 °C, anode and cathode flow rates of 28.8 LPM H₂+5 LPM N₂ and 72 LPM air, respectively. The open circuit voltage of the stack reached to 43.96 V (1.22 V/cell). While the operating current set at 32 A and stack voltage at 33.1 V (average cell voltage 0.92 V/cell), the electric power output was 1069 W. As

the anode and cathode flow rates were decreased to 18 LPM H₂+5 LPM N₂ and 60 LPM air, respectively, the power output slightly decreased to 1043 W at the same current density. Meanwhile, the fuel utilization and power efficiency were 48.7% and 35.4%, respectively. Figure 11 shows the current, voltage and power curves for the stack. The voltage variations among cells are illustrated in Figure 12.

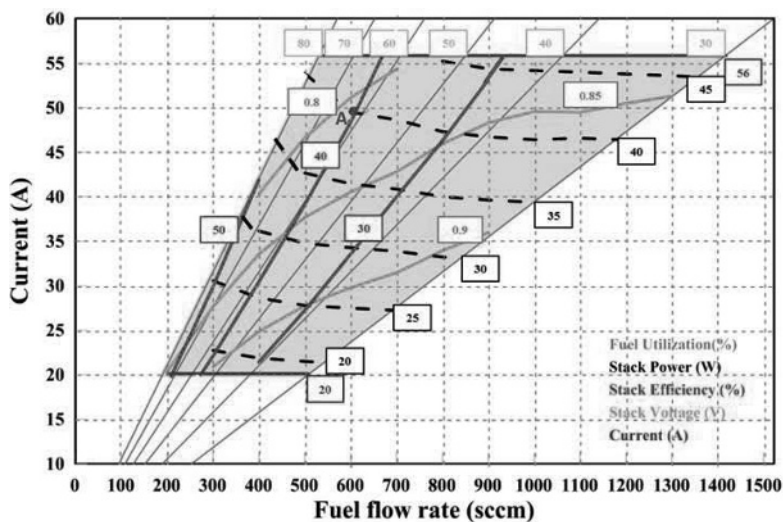


Figure 10. Performance map for a single-cell stack.

Table 1 Operating parameters and ranges for a single-cell stack.

Parameters	Operating ranges
Fuel flow rate (sccm)	200~1400
Current (A)	20~50
Stack voltage (V)	0.8~0.9
Stack power (W)	20~45
Fuel utilization (%)	30~80
Electric efficiency (%)	30~50

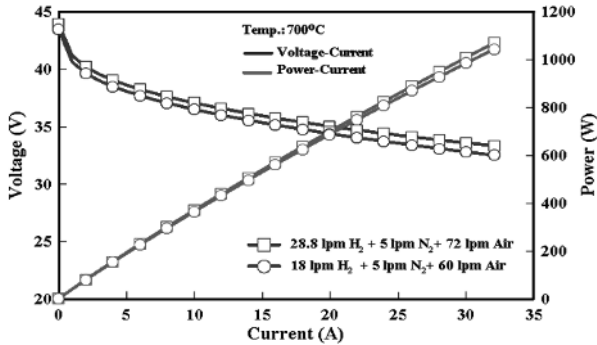


Figure 11. I-V-P curves of the 36-cell stack under different gas flow rates.

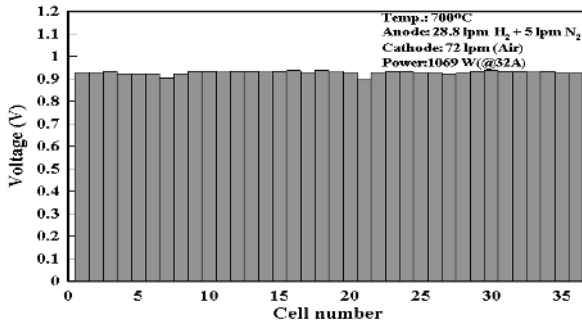


Figure 12. Variations of cell voltages of the 36-cell stack operated at 1069W

SYSTEM DEVELOPMENT

Innovative nano-structure catalysts, ceria (CeO_2)-assisted Pt catalysts coated on a modified, tablet-shape $\alpha\text{-Al}_2\text{O}_3$ support ($\text{Pt/CeO}_2/\alpha\text{-Al}_2\text{O}_3$), were developed. Performance test for the catalysts was carried out to illustrate its high resistance of coking and pulverization as well as its high conversion rate for auto-thermal reforming (ATR) of the natural gas.^{34,35} The reforming catalyst was able to function continuously and remained at a methane conversion rate higher than 90% during the 4000-hour durability test. As different configurations of the carrier substrates might significantly impact the catalyst performance, attentions have to be devoted to various types of catalyst structures, e.g. powders, tablets, honeycombs, foams, etc.³⁶⁻⁴⁰ Additionally, the use of precious metal in the catalyst layer should be properly minimized to lower the cost of raw materials while maintaining good natural gas reforming performance. In the present study, to cope with different system configurations for a satisfactory reforming efficiency, a new type of ring-shape carriers with different Pt contents were tested to investigate their performance on steam reforming of natural gas at 800°C. Figure 13 indicates the XRD pattern for the 12% $\text{CeO}_2/\alpha\text{-Al}_2\text{O}_3$ with different amount of Pt contents. Comparisons of methane conversion rates using ring-shape supported carriers with various Pt contents at 800°C are illustrated in Figure 14. As both the cost and performance of the catalyst are taken into accounts, among the

tested catalysts, the one with 0.5%Pt/12%CeO₂/α-Al₂O₃ composition could be a proper selection for the time being.

For the system development, the kilowatt grade SOFC system is preliminarily pursued to develop the core technologies for a power system. As the first prototype power system (INER-I) was demonstrated in 2011, efforts have been devoted to reducing the system volume, enhancing the control logics and I&C diagnosis and improving the safety for the system. The hot components of the balance of plant, such as afterburner, reformer, evaporator and heat exchanger were sequentially integrated into a hot module. Startup procedures were prudently examined so that the power system could be heated up through interior thermal management. As a result, the system volume of the INER-III is effectively reduced to 36% of the original prototype (INER-I). A planar 36-cell stack, as aforementioned in the previous paragraph, was installed onto the INER-III power system for system validation tests. The system was heated up by the thermal energy from the afterburner. Validation test was carried out with the hydrogen as fuel to check its consistency with the result of stack testing. Then, a steady 600-hour system operation test was carried out to validate the stability of the SOFC power system. As the reformer of the system was operated with partial oxidation mode, the steam to carbon (S/C) and oxygen to carbon (O/C) ratios were set to 1.7 and 0.3, respectively. Experimental data indicated the average stack temperature was 693 °C, and the current, stack voltage and power were 36 A, 29.48 V, and 1060 W, respectively. The fuel utilization and electric efficiency were then calculated to be 67.16% and 45%, respectively. Another test conditions, the power system was operated under steam reforming plus water gas shift reactions. In this case, the S/C ratio was set to 2.0 and the average stack temperature was 696 °C. As the current was 36 A, the average stack voltage and power were respectively 28.74 V and 1063 W. Meanwhile, the fuel utilization and electric efficiency were 53.65% and 42.4%, respectively. Figure 15 shows the I-V-P curves for these tests.

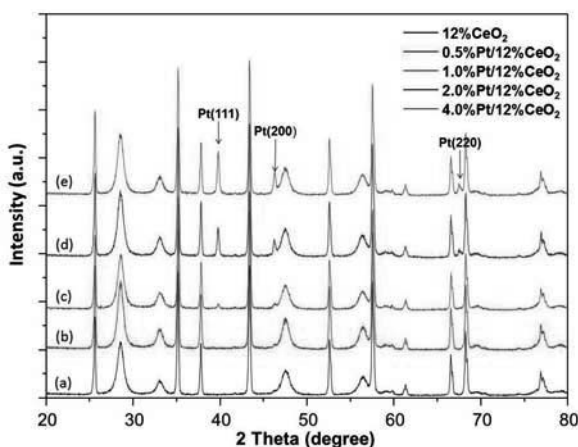


Figure 13. XRD patterns of (a) 12%CeO₂/α-Al₂O₃, (b) 0.5%Pt/12%CeO₂/α-Al₂O₃, (c) 1.0%Pt/12%CeO₂/α-Al₂O₃, (d) 2.0%Pt/12%CeO₂/α-Al₂O₃, and (e) 4.0%Pt/12%CeO₂/α-Al₂O₃.

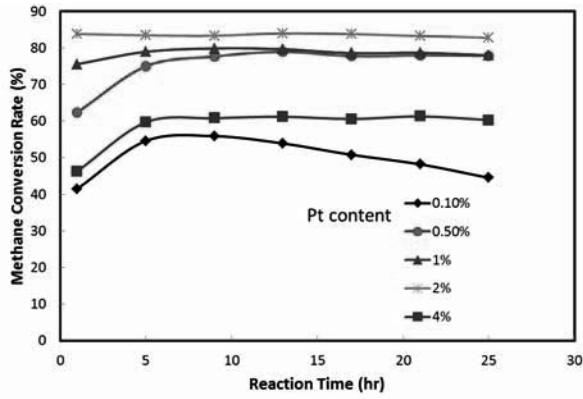


Figure 14. Comparisons of methane conversion rates using ring-shape supported catalysts with various Pt contents at 800°C.

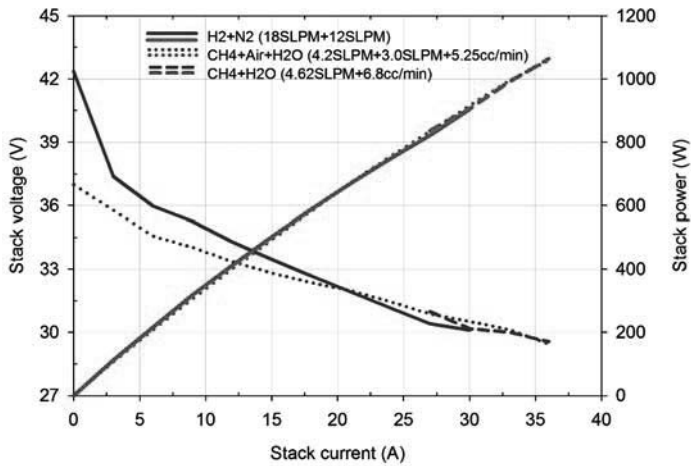


Figure 15. I-V-P curves of a 36-cell stack on the INER-III SOFC system.

Table 2. Experimental results for the INER-III SOFC power system.

Experimental conditions	Gas flow rate in LPM H ₂ O in cc/min	OCV (V)	Stack power	Fuel utilization (%)	Electrical eff. (%)
Dilute gas H ₂ +N ₂	H ₂ : 16 N ₂ : 13	42.35	933 W (@31A)	53.13	36.0
Steam reforming+ partial oxidation+ water gas shift (SR+POX+WGS)	CH ₄ :4.6 Air:3.04 H ₂ O:5.78	36.98	1060 W (@36A)	67.16	45.0
Steam reforming+ water gas shift (SR+WGS)	CH ₄ :4.6 H ₂ O:6.8	36.98	1063 W (@36A)	53.65	42.4

CONCLUSION

After the elaborative efforts for over a decade, substantial progresses have been made at INER in cell, stack and power system developments. Some remarks are listed as follows:

- Cell: Technology for both the ASC and MSC cells is developed with a power density higher than 500 mW/cm² and a degradation rate around 1%/khr.
- Sealant: A proprietary barium-aluminum-borosilicate glass, designated as GC9, is employed as a high-temperature seal. The hybrid sealants, such as phlogopite mica/GC9, are investigated to improve the thermal and mechanical properties as well as durability to widen its SOFC applications.
- Stack: Standard operational procedures are made for stacking, curing and test protocols. Consistent and repeatable test results are achieved for SOFC stacks. The deviation of cell voltages is within 2% for a 36-cell stack operating at 1 kW.
- System: a compact INER-III power system, where its volume is 36% of the origin prototype INER-I, has been demonstrated with electric efficiency higher than 40% as the natural gas is employed as fuel.

Continuous improvements are under way for a reliable and high performance SOFC product. It is hoped that through technology transfers and intensive collaborations with industry partners would be beneficial to the commercialization of the SOFC technology to the viable markets in the near future.

ACKNOWLEDGMENT

The authors would like to acknowledge the strong supports from the INER's management officers and team members in the INER's SOFC Project for their persistent efforts on the development of SOFC technology.

REFERENCES

- ¹ R. Y. Lee, Y. N. Cheng, C. S. Hwang, M. C. Lee, N. Y. Hsu and W. T. Hong, Development of solid oxide fuel cell technology at the Institute of Nuclear Energy Research, *Journal of Physical Science and Application* 3, 2013, 175-183.
- ² R. Y. Lee, Y. N. Cheng, W. T. Hong, N. Y. Hsu, C. S. Hwang, T. N. Lin, M. C. Lee, and L. F. Lin, Overview and perspective of SOFC technology development in Taiwan, 11th European SOFC & SOE Forum, Chapter 02, A0302, 2014, 7-15.
- ³ M. C. Lee, T. N. Lin and R. Y. Lee, Development and application of SOFC-MEA technology at INER, *Advances in Solid Oxide Fuel Cells: Ceramic Engineering and Science Proceedings*, *Advances in Solid Oxide Fuel Cells IX: Ceramic Engineering and Science Proceedings*, 2013, Vol. 34, pp. 41-65.
- ⁴ C. L. Chang, C. S. Hwang, C.H. Tsai, C.M. Chuang, S.W. Cheng, S.H. Wu and S. H. Nien, Development of Plasma Sprayed Metal-Supported solid oxide fuel cells at Institute of Nuclear Energy Research, *Advances in Solid Oxide Fuel Cells and Electronic Ceramics IX: Ceramic Engineering and Science Proceedings*, 2013, Vol. 34, pp. 31-39.
- ⁵ T.N. Lin, M.C. Lee, R.Y. Lee, Synthesis of $\text{SmBa}_{0.5}\text{Sr}_{0.5}\text{Co}_2\text{O}_{5+\delta}$ powder and its application as composite cathode for intermediate temperature solid oxide fuel cell, *Advances in Solid Oxide Fuel Cells: Ceramic Engineering and Science Proceedings*, *Advances in Solid Oxide Fuel Cells X: Ceramic Engineering and Science Proceedings*, 2014, Vol. 35, pp. 55-64.
- ⁶ T.N. Lin, Y. C. Chang, M.C. Lee, and R.Y. Lee, Fabrication of anode-supported oxide fuel cell with composite cathodes and the performance evaluation upon long term operation, *Advances in Solid Oxide Fuel Cells: Ceramic Engineering and Science Proceedings*, *Advances in Solid Oxide Fuel Cells X: Ceramic Engineering and Science Proceedings*, 2015, Vol. 36, pp. 83-92.
- ⁷ C.H. Wang, M.C. Lee, Y.C. Chang, W.X. Kao, T.N. Lin, Process to produce fine ceramic powder through a chemical reactor with powder collection device, US patent No. US8,287,813B2 (2012.10.16) / ROC Patent No. I 405609 (2013.08.21).
- ⁸ Y.C. Chang, M.C. Lee, W.X. Kao, C.H. Wang, T.N. Lin, J.C. Chang, and R.J. Yang, Characterizations of the anode-supported solid-oxide fuel cells with an yttria stabilized zirconia thin film by the diagnosis of the electrochemical impedance spectroscopy, 2011, *J. Electrochemical Soc.*, 158(3), B259-B265.
- ⁹ W.X. Kao, M.C. Lee, T.N. Lin, C.H. Wang, and Y.C. Chang, Fabrication and characterization of $\text{Ba}_{0.5}\text{Sr}_{0.5}\text{Co}_{0.8}\text{Fe}_{0.2}\text{O}_{3-\delta}$ -GDC cathode for anode supported SOFC, 2011, *Journal of Power Sources*, Vol. 195, 2220-2223.
- ¹⁰ J.C. Chang, M.C. Lee, R.J. Yang, Y.C. Chang, T.N. Lin, C.H. Wang, W.X. Kao, and L.S. Lee, Fabrication and characterization of SDC-SSC composite cathode for anode supported Solid Oxide Fuel Cell, 2011, *Journal of Power Sources*, 196, 3129-3133.
- ¹¹ T.N. Lin, M.C. Lee, R.J. Yang, J.C. Chang, W.X. Kao, L.S. Lee, Chemical state identification of $\text{Ce}^{3+}/\text{Ce}^{4+}$ in the $\text{Sm}_{0.2}\text{Ce}_{0.8}\text{O}_{2-\delta}$ electrolyte for an anode-supported solid oxide fuel cell after long-term operation, 2012, *Materials Letters*, 81, 185-188.
- ¹² C.S. Hwang, C.H. Tsai, C.H. Lo and C.H. Sun, Plasma sprayed metal supported YSZ/Ni-LSGM-LSCF ITSOFC with nanostructured anode, *J. Power Sources*, 180 132-142 (2008).
- ¹³ J. W. Fergus, Review – Sealants for solid oxide fuel cells, *J. Power Sources*, 147, 46-57 (2005).
- ¹⁴ M. K. Mahapatra and K. Lu, Glass-based seals for solid oxide fuel and electrolyzer cells – A review, *Mater. Sci. Eng. R.*, 67(5-6), 65-85 (2010).
- ¹⁵ D. U. Tulyaganov, A. A. Reddy, V. V. Kharton, and J. M. F. Ferreira, Aluminosilicate-based sealants for SOFCs and other electrochemical applications – A brief review, *J. Power Sources*, 242, 486-502 (2013).
- ¹⁶ C. K. Liu, T. Y. Yung, K. F. Lin, R. Y. Lee, and T. S. Lee, Glass-ceramic sealant for planar

solid oxide fuel cells, United States Patent No. 7,897,530 B2 (2011).

¹⁷ S. H. Wu, K. F. Lin, R. Y. Lee, C. K. Liou, T. Y. Yung, T. S. Lee, and L. C. Cheng, Sealing material for solid oxide fuel cells, United States Patent No. 8,012,895 B2 (2011).

¹⁸ C. K. Liu, T. Y. Yung, K. F. Lin, R. Y. Lee, and S. H. Wu, High temperature glass-ceramic seals for SOFC applications, ECS Trans., 25(2), 1491-1500 (2009).

¹⁹ C. K. Liu, K. F. Lin, and R. Y. Lee, Characteristics of the sintered phlogopite mica/SiO₂-B₂O₃-Al₂O₃-BaO-La₂O₃ glass blends, ECS Trans., 35(1), 2519-2526 (2011).

²⁰ C. K. Liu, R. Y. Lee, K. C. Tsai, S. H. Wu, and K. F. Lin, Characterization and performance of a high-temperature glass sealant for solid oxide fuel cell, Advances in Solid Oxide Fuel Cells X, 35(3), 65-75 (2014).

²¹ C. K. Liu, K. F. Lin, and R. Y. Lee, Effects of lanthanum-to-calcium ratio on the thermal and crystalline properties of BaO-Al₂O₃-B₂O₃-SiO₂ based glass sealants for solid oxide fuel cells, J. Ceram. Soc. Japan, 123(1436), 239-244 (2015).

²² H. T. Chang, C. K. Lin, and C. K. Liu, High-temperature mechanical properties of a glass sealant for solid oxide fuel cell, J. Power Sources, 189(2), 1093-9 (2009).

²³ H. T. Chang, C. K. Lin, and C. K. Liu, Effects of crystallization on the high-temperature mechanical properties of a glass sealant for solid oxide fuel cell, J. Power Sources, 195(10), 3159-65 (2010).

²⁴ H. T. Chang, C. K. Lin, C. K. Liu, and S. H. Wu, High-temperature mechanical properties of a solid oxide fuel cell glass sealant in sintered forms, J. Power Sources, 196(7), 3583-91 (2011).

²⁵ C. K. Lin, K. L. Lin, J. H. Yeh, W. H. Shiu, C. K. Liu, and R. Y. Lee, Aging effects on high-temperature creep properties of a solid oxide fuel cell glass-ceramic sealant, J. Power Sources, 241(1), 12-9 (2013).

²⁶ C. K. Lin, K. L. Lin, J. H. Yeh, S. H. Wu, and R. Y. Lee, Creep rupture of the joint of a solid oxide fuel cell glass-ceramic sealant with metallic interconnect, J. Power Sources, 245, 787-795 (2014).

²⁷ C. K. Lin, W. H. Shiu, S. H. Wu, C. K. Liu, and R. Y. Lee, Interfacial fracture resistance of the joint of a solid oxide fuel cell glass-ceramic sealant with metallic interconnect, J. Power Sources, 261(1), 227-237 (2014).

²⁸ C. K. Lin, Y. A. Liu, S. H. Wu, C. K. Liu, and R. Y. Lee, Joint strength of a solid oxide fuel cell glass-ceramic sealant with metallic interconnect in a reducing environment, J. Power Sources, 280, 272-288 (2015).

²⁹ S.W. Cheng, Y.H. Shiu, Y. N. Cheng, and R.Y. Lee, Measurements of lateral impedance and local characteristics of solid oxide fuel cells, J. Fuel Cell Science and Technology, Vol. 9 Issue 4, (2012).

³⁰ Y. N. Cheng, S.W. Cheng, and R.Y. Lee, The comparisons of electrical performance and impedance spectrum for two commercial cells, INT. J. Hydrogen Energy, Vol. 11, Oct., (2014).

³¹ S.W. Cheng, C.H. Tsai, S. H. Wu, C. K. Liu, Y. N. Cheng, and R.Y. Lee, Effects of reduction process on the electrochemical and microstructural properties for electrolyte-supported SOFC, INT. J. Hydrogen Energy, Vol. 40, 1534-1540 (2015).

³² J.K Lin, S.W Cheng, C.W Lu, Y.N Cheng, R.Y Lee, and H.Y Kuo, T.N Lin, Application of Taguchi method to optimize the operating parameters for commercial Solid Oxide Fuel Cell, Key Engineering Materials Vols 656-657, p.p. 544-548 (2015).

³³ C.W Lu, S.H Wu, H.H Lin, W.H Chung, J.K Lin, Y.N Cheng, and R.Y Lee, Optimization of operating conditions for an SOFC stack, Key Engineering Materials Vols 656-657, p.p. 119-123 (2015).

³⁴ N. Y. Hsu and K. T. Jeng, Reforming of natural gas using coking-resistant catalyst for fuel cell system applications, Journal of Power Sources 222, p.p. 253-260 (2013).

³⁵ N. Y. Hsu, K. T. Jeng, S. D. Chiou, S. H. Lin, H. Y. Tzeng, W. M. Huang, Y. M. Chang, and R.

Y. Lee, Method of modifying nano-porous gas reforming catalyst with high temperature stability, US. Patent Application No. 13/657,996, (granted Dec. 2015.)

³⁶ D.-J. Liu, et al., Characterization of kilowatt-scale autothermal reformer for production of hydrogen from heavy hydrocarbons, *International Journal of Hydrogen Energy* 29, 1035–1046 (2004).

³⁷ A. Beretta, et al., Optimal design of a CH₄ CPO-reformer with honeycomb catalyst: combined effect of catalyst load and channel size on the surface temperature profile, *Catalysis Today* 171 (1,) 79–83 (2011).

³⁸ P. Ciambelli, V. Palma, E. Palo, Comparison of ceramic honeycomb monolith and foam as Ni catalyst carrier for methane autothermal reforming, *Catalysis Today* 155 (1–2) (2010) 92–100.

³⁹ S. Kado, et al., Syngas production from natural gas via catalytic partial oxidation using ceramic monolith catalyst at short contact time and elevated pressure, *Catalysis Today* 171 (1), 97–103 (2011).

⁴⁰ Vincenzo Palma, Antonio Ricca, Paolo Ciambelli, Methane auto-thermal reforming on honeycomb and foam structured catalysts: The role of the support on system performances, *Catalysis Today* 216, 30–37(2013).

